

Numerical Investigation of the Recirculation Zone Length Upstream of the Round-Nosed Broad Crested Weir

Mehmet Anıl Kızılaslan¹, Ender Demirel²

^{1,2}Department of Civil Engineering, Eskisehir Osmangazi Univesity, 26480 Eskisehir, Turkey

Abstract: *Broad crested weirs (BCW) are widely used hydraulic structures in streams and irrigation channels to control the flow and to measure the discharge due to the advantage of having simple geometry. Interaction of the turbulent flow with the structure generates vortices and recirculation zone upstream of the weir, which may cause significant morphological changes on the stream bed. In this study, flow structure upstream of the round-nosed BCW is investigated based on two-dimensional Unsteady Reynolds-Averaged Navier-Stokes Simulations (URANS). Numerical simulations are conducted using OpenFOAM for different flow rates and rounding parameters of the weir. The Shear Stress Transport (SST) $k-\omega$ turbulence model is employed in order to calculate the adverse pressure gradients and separation effects accurately on the channel bottom and weir crest. Numerical results are reported and interpreted with focus on the effect of rounding on the length of the recirculation zone.*

Keywords: *Broad crested weir, recirculation zone length, OpenFOAM, turbulence, free-surface.*

1. Introduction

Round-nosed BCWs can be used in field and laboratory channels for flow measurement because of their good range of discharge and high modular limit (Ramamurthy et. Al., 1988). The flow pattern over BCW is still up to date due to the existence of complex flow structure near the weir. Sarker and Rhodes (2004) carried out numerical and experimental studies for the investigation of flow structure upstream and downstream of a rectangular BCW. Free-surface profiles were measured by using pointer-gauge in their experimental study. They used Fluent software for the simulation of turbulent flow based on Reynolds Average Navier Stokes (RANS) equations and Volume of Fluid (VOF) method was used to capture the position of the free-surface. Gonzales and Chanson (2007) used four different BCW geometries to determine the velocity and pressure profiles experimentally. They observed an effective recirculation zone upstream of the weir which is associated with the turbulent boundary layer. Zachoval and Rousar (2015) investigated the flow structure upstream of a BCW experimentally using Ultrasonic Velocity Profile (UVP) and Particle Image Velocimetry (PIV) to determine the flow pattern. Hargreaves et. al. (2007) used different turbulence models to investigate the free-surface profile over a BCW. They compared numerical results with the experimental results available in the literature showing that the separation zone could be calculated accurately by the $k-\epsilon$ turbulence model. Modammadpour et. al. (2013) carried out numerical simulations on a gabion type porous weir to investigate the flow pattern. Kirkgoz et. al. (2008) conducted numerical and experimental studies to determine the flow pattern upstream of broad crested and v-notch weirs. Numerical simulations were carried out by using a ANSYS (2009) based on the standard $k-\epsilon$ and $k-\omega$ turbulence closure models. Haun et. al. (2014) simulated flow over a BCW with two different numerical solvers, namely FLOW 3D and SSIM 2 and they compared the numerical results consistently. Gogus et. al. (2006) carried out experimental studies for the effect of threshold height on the approach velocity coefficient, modular limit and discharge coefficient for BCW. Ramamurthy et. al. (1988) conducted experimental studies to propose a discharge coefficient as a function of nose radius, weir height and water depth for both free and submerged flow conditions. Felder and Chanson (2012) carried out experimental studies to measure the free-surface, pressure and

velocity profiles on a round-nosed BCW. They observed a recirculation zone at the end of the weir. Zachoval et al. (2012) investigated the flow separation on the upstream corner of a rectangular BCW.

Aforementioned studies generally focused on discharge coefficient, flow pattern and free-surface profiles. Complex flow structure near the weir forms recirculation zones at both upstream and downstream of the weir, which can be responsible for the morphological changes on the river bed. In this study, the length of the recirculation zone examined numerically for distinct dimensionless rounding parameters of R/P and flow rates. Numerical simulations are conducted using OpenFOAM and the SST $k-\omega$ turbulence closure model is employed in order to calculate the adverse pressure gradients and separation effects on the walls accurately.

2. Numerical Modelling

In Computational Fluid Dynamics (CFD), the $k-\omega$ turbulence model is a common two-equation turbulence model, that is used as a closure for the Reynolds-Averaged-Navier-Stokes (RANS) equations. In this study, Wilcox's (2006) version of $k-\omega$ model equations were used, which are defined as the following governing equations (OpenFOAM, 2015):

$$\frac{\partial k}{\partial t} + \bar{u}_j \frac{\partial k}{\partial x_j} = P - \beta^* \omega k + \frac{\partial}{\partial x_j} \left[\left(\nu + \sigma_k \frac{k}{\omega} \right) \frac{\partial k}{\partial x_j} \right] \quad (1)$$

$$\frac{\partial \omega}{\partial t} + \bar{u}_j \frac{\partial \omega}{\partial x_j} = \frac{\gamma \omega}{k} P - \beta \omega^2 + \frac{\partial}{\partial x_j} \left[\left(\nu + \sigma_k \frac{k}{\omega} \right) \frac{\partial k}{\partial x_j} \right] + \frac{\sigma_d}{\omega} \sigma_k \frac{\partial k}{\partial x_j} \frac{\partial \omega}{\partial x_j} \quad (2)$$

where;

$$P = \tau_{ij} \frac{\partial \bar{u}_i}{\partial x_j} \quad (3)$$

$$\tau_{ij} = 2\nu S_{ij} - \frac{2}{3} k \delta_{ij} \quad (4)$$

$$S_{ij} = \frac{1}{2} \left(\frac{\partial \bar{u}_i}{\partial x_j} + \frac{\partial \bar{u}_j}{\partial x_i} \right) \quad (5)$$

$$\nu_t = \frac{k}{\omega} \quad (6)$$

Where, ν_t is eddy viscosity, ω is turbulent dissipation rate, k is the turbulent energy, τ_{ij} is turbulent Reynolds stress tensor, β^* and γ are turbulence modelling constants, S_{ij} mean rate of deformation components. Details of the numerical model can be found in (Wilcox, 2006).

2.1 Numerical Setup

OpenFOAM is an open source CFD toolbox that enables to modify the standard solvers and develop novel boundary conditions. A custom boundary condition was implemented at the inlet to reduce the length of the computational domain and time. The following parabolic velocity distribution is applied at the inlet of the computational domain (Cassan and Belaud, 2012):

$$U(y) = (\gamma + 1) U_0 \left(\frac{y}{h_0} \right)^\gamma \quad (7)$$

Where γ is shape factor which is set to 0.1 in this study, U_0 is the area averaged horizontal velocity component at the inlet, which can be calculated from the flow rate and water depth (h_0).

Geometry and computational mesh were generated using *blockMesh* utility which is available in OpenFOAM. Computational mesh is clustered in the vicinity of the bottom of the channel, rounded upstream corner, top of the weir and free-surface in order to capture severe variations in flow quantities accurately. As shown in Fig.1, non-orthogonality of the mesh increases near the rounded nose to fit the mesh to the circular

wall. Thus, non-orthogonal correction needs to be applied during numerical solution in order to obtain converged results in both velocity and pressure fields accurately.

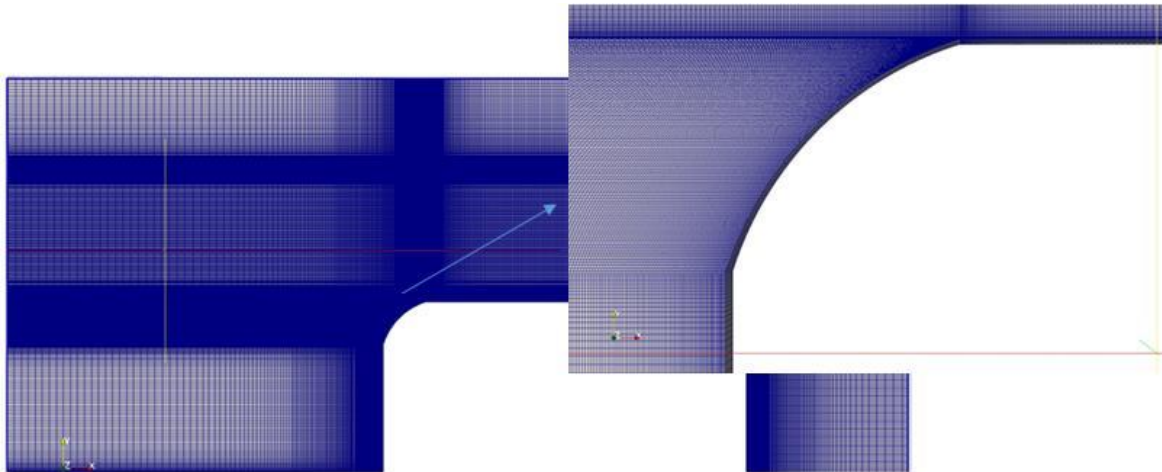


Fig. 1: Different views of non-orthogonal variable mesh.

In this study, four different rounding parameters were selected as shown in Table 1, in order to investigate the effect of rounding on the recirculation zone length. Numerical simulations were performed for different flow rates of $Q=15, 45, 85$ and 125 lt/s over a broad-crested weir with dimensions of $P=37.5$ cm, $L=80$ cm as shown in Fig. 2. Thus, effects of rounding and flow discharge on the development of recirculation zone will be examined based on the numerical simulation results for steady state flow field.

TABLE I: Rounding parameters in numerical simulations.

Case	R/P
Case1	0.02
Case2	0.0094
Case3	0.1876
Case4	0.25

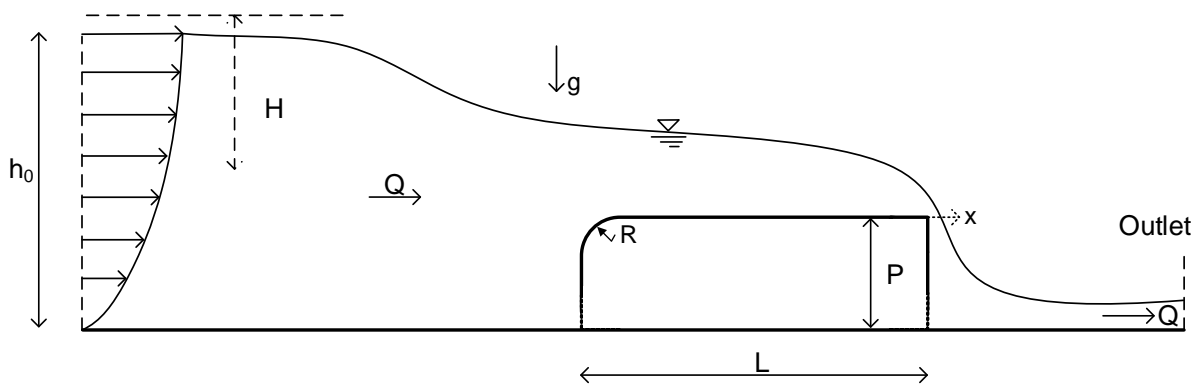


Fig. 2: Schematic view of the BCW.

Numerical simulations were performed during 100 seconds in each computational run in order to avoid the effects of initial conditions and to obtain time-averaged flow data. It should be noted that adequate data needs to be collected during the simulations to obtain time-averaged flow field which is required to plot the streamlines at the post-processing step. Preliminary numerical simulation results showed that free-surface height and velocity

remained unchanged after 100 seconds even though the flow discharge exceeds the maximum value of 125 lt/s, which is acceptable for the present problem.

The Reynolds number for the present problem is defined in Equation (8) and calculated Reynolds numbers are listed in Table 1 for each case. Corresponding Reynolds numbers show that the flow is fully turbulent.

$$Re = \frac{H\sqrt{gH}}{\nu} \tag{8}$$

in which Re is the Reynolds number of the flow, ν is the kinematic viscosity of the fluid, H is the energy head over the weir. Boundary conditions for the turbulence are calculated and applied at the inlet of the channel based on the %5 intensity of the turbulence as shown in Table II, which is common for fully developed open channel flows.

TABLE II: Numerical parameters for Case1

Q (lt/s)	Re	k	ω	Number of mesh
15	106397	2.39E-5	5.43	317496
45	308214	1.34E-4	6.62	317496
85	580484	3.4E-4	7.04	317496
125	730319	6.3E-4	7.59	317496

3. Results and Discussion

In this study, flow structure upstream of the round-nosed BCW is investigated based on two-dimensional Unsteady Reynolds-Averaged Navier-Stokes (URANS) simulations. Numerical simulations are conducted using OpenFOAM. The Shear Stress Transport (SST) $k-\omega$ turbulence model is employed in order to calculate the adverse pressure gradients and separation effects on the walls accurately. Numerical simulations were performed on a rectangular channel with having 2.2 m upstream length. The length of the recirculation zone is determined based on the horizontal velocity profiles and streamline patterns at the post-processing step. Horizontal velocity profiles at different locations are plotted in Fig. 3 for $R/P=0.02$ and $R/P=0.25$. The velocity of the fluid is significantly affected by the radius of the nose as shown in Fig. 3b.

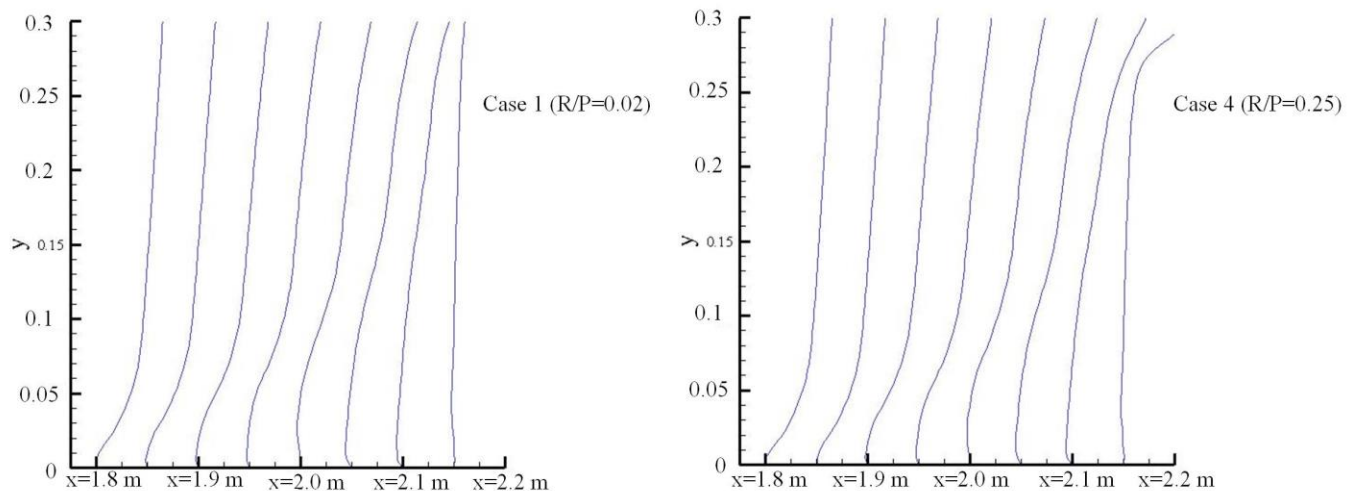


Fig. 3. Horizontal velocity profiles for $R/P=0.02$ and $R/P=0.25$.

It can be seen in Fig.3 that the backward effects upstream of the weir increase as the radius of the weir increases. The rounding of the upstream nose strongly affects the flow field near the weir. Streamline patterns

are given in Fig. 4 for the flow rates $Q=15$ and 125 lt/s and rounding $R/P=0.02$ and 0.25 . The length of the recirculation is obtained from Fig.4 by digitizing the flow data. Length of the recirculation zone is determined as 57.5 cm for $Q=15$ lt/s. It is clearly seen from the figure that the length of the recirculation zone decreases when the R/P increases due to fact that separation effects on the rounded nose decreases when the rounding increases. Recirculation zones are calculated for each case and listed in Table III.

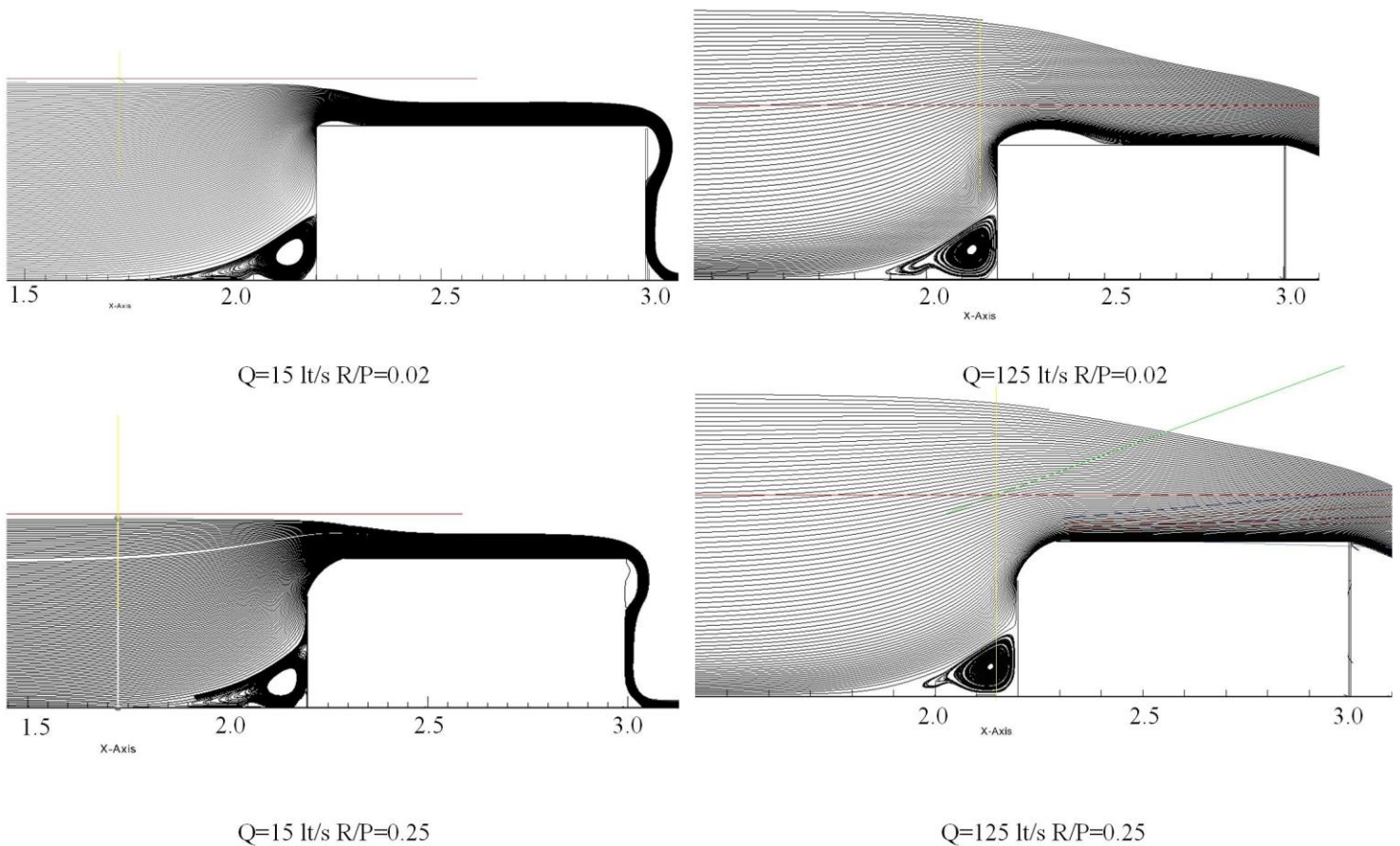


Fig. 4. Streamlines for $Q=15$ and 125 lt/s.

The following conclusions can be drawn based on the results listed in Table III:

1. The length of the recirculation zone decreases as the rounding of the nose increases for a fixed flow rate which may be associated with the separation effects on the bed. The separation on the channel bottom decreases when the rounding of the nose increases since the flow discharge capacity of the weir has increased. This observation points out that morphological changes associated with the recirculation effects may be critical for the weirs having square edged upstream corner.
2. Flow rate is not as much effective as the rounding on the development of the recirculation zone. If we consider the case having minimum rounding, the length of the recirculation zone decreases when the flow rate increases. However, the length of the recirculation zone starts to increasing surprisingly when the flow rate becomes 125 lt/s. This may be due to that the effect of separation on the bed becomes significant after a certain value of Reynolds number.
3. Separation of the flow on the crest produces an additional dead zone for small values of rounding as seen in Fig.4. Moreover, the length of the recirculation zone on the crest increases as the flow rate increases. This proves that the flow discharge capacity of the weir reduces when the rounding of the nose decreases.
4. A sudden drop is observed at the entrance of the crest and it vanishes as the rounding of the weir increases.

TABLE III: Recirculation zone lengths

Q (lt/s)	Case	Nose Rounding (cm)	Recirculation zone length (m)
15	Case1	0.75	0.575
	Case2	3.525	0.5125
	Case3	7.035	0.4923
	Case4	9.375	0.3856
45	Case1	0.75	0.5436
	Case2	3.525	0.45
	Case3	7.035	0.3874
	Case4	9.375	0.346
85	Case1	0.75	0.5086
	Case2	3.525	0.4857
	Case3	7.035	0.3446
	Case4	9.375	0.31
125	Case1	0.75	0.5462
	Case2	3.525	0.493
	Case3	7.035	0.378
	Case4	9.375	0.341

4. References

- [1] ANSYS FLUENT 12.0 Theory Guide, ANSYS Inc, 2009.
- [2] Cassan, L., Belaud, G. "Experimental and Numerical Investigation of Flow under Sluice Gates", *Journal of Hydraulic Engineering*, 138, 367-373., 2012.
[https://doi.org/10.1061/\(ASCE\)HY.1943-7900.0000514](https://doi.org/10.1061/(ASCE)HY.1943-7900.0000514)
- [3] Göğüş, M., Defne, Z., Özkandemir, V., "Broad-Crested Weirs with Rectangular Compound Cross Sections", *Journal of Irrigation and Drainage Engineering*, 132(3), 272-280, 2006.
[https://doi.org/10.1061/\(ASCE\)0733-9437\(2006\)132:3\(272\)](https://doi.org/10.1061/(ASCE)0733-9437(2006)132:3(272))
- [4] Hargreaves, D. M., Morvan, H.P., Wright, N.G. "Validation of the Volume of Fluid Method for Free Surface Calculation: The Broad Crested Weir", *Engineering Applications of Computational Fluid Mechanics*, 1(2), 136-146, 2007.
<https://doi.org/10.1080/19942060.2007.11015188>
- [5] Haun, S., Olsen, N.R.B., Feurich, R. "Numerical Modeling of Flow Over Trapezoidal Broad-Crested Weir", *Engineering Applications of Computational Fluid Mechanics*, 5(3), 397-405, 2011.
<https://doi.org/10.1080/19942060.2011.11015381>
- [6] Kirkgoz, M.S., Akoz, M.S., Oner, A.A. "Experimental and Theoretical Analyses of Two-Dimensional Flows Upstream of Broad-Crested Weirs", *Canadian Journal of Civil Engineering*, 35, 975-986, 2008.
<https://doi.org/10.1139/L08-036>
- [7] Mohammadpour, R., Ghani, A.A., Azamathulla, H.M. "Numerical Modeling of 3-D Flow Porous Broad Crested Weirs" *Applied Mathematical Modelling*, 37, 9324-9337, 2013.
<https://doi.org/10.1016/j.apm.2013.04.041>
- [8] OpenFOAM, The OpenFOAM Foundation; OpenCFD Ltd.:Bracknell, UK, 2015.
- [9] Ramamurthy, A.S., Tim, U.S., Rao, M.V.J. "Characteristics of Square-Edged and Round-Nosed Broad-Crested Weirs", *Journal of Irrigation and Drainage Engineering*, 114, 61-73, 1988.
[https://doi.org/10.1061/\(ASCE\)0733-9437\(1988\)114:1\(61\)](https://doi.org/10.1061/(ASCE)0733-9437(1988)114:1(61))
- [10] Sarker, M.A., Rhodes, D.G. "Calculation of Free-Surface Profile Over a Rectangular Broad-Crested Weir", *Flow Measurement and Instrumentation*, 15, 215-219, 2004.
<https://doi.org/10.1016/j.flowmeasinst.2004.02.003>

- [11]Zachoval, Z., Roušar, L. “Flow Structure in front of the Broad-Crested Weir”, EPJ Web of Conferences, 92, 02117.2015.
<https://doi.org/10.1051/epjconf/20159202117>